8-2018

Functionalization of Hyaluronic Acid Hydrogels with ECM-derived Peptides to Control Myoblast Behavior

Juan Martin Silva Garcia
Purdue University

FUNCTIONALIZATION OF HYALURONIC ACID HYDROGELS WITH ECM-DERIVED PEPTIDES TO CONTROL MYOBLAST BEHAVIOR

by

Juan Martin Silva Garcia

A Thesis

Submitted to the Faculty of Purdue University

In Partial Fulfillment of the Requirements for the degree of

Master of Science in Biomedical Engineering

Weldon School of Biomedical Engineering

West Lafayette, Indiana

August 2018

THE PURDUE UNIVERSITY GRADUATE SCHOOL
STATEMENT OF COMMITTEE APPROVAL

Dr. Sarah Calve, Chair
Department of Biomedical Engineering
Dr. Alyssa Panitch
Department of Biomedical Engineering
Dr. Luis Solorio
Department of Biomedical Engineering

Approved by:

Dr. George R. Wodicka
Head of the Graduate Program

This work is dedicated to my beloved family who supported me with no hesitation during this important phase of my life. Thank you God for placing me in the right time and place with amazing people.

ACKNOWLEDGMENTS

There have been many people who have walked alongside me during this process. They have guided me, placed opportunities in front of me and showed me the doors that might be useful to open. I would like to thank Dr. Sarah Calve and Dr. Alyssa Panitch, without your encouragement the road would have seemed a lonely place.

Nimisha Bajaj for being so patient and supportive during challenging times. Maria de la Luz Garcia Issais for believing in me and encouraging me to always be better than the surrounding circumstances and teaching me to appreciate the precious opportunities that were and are still given to me. SabasX2 for being there, giving me always the support and help needed.

Finally, the Calve and Panitch lab which made this years an amazing journey.

TABLE OF CONTENTS

LIST OF TABLES

LIST OF FIGURES

LIST OF ABBREVIATIONS

Dithiobis Propanoic Dihydrazide	DTPH
Extracellular Matrix	ECM
Hyaluronic Acid	HA
Polyethylene Glycol Diacylate	PEGDA
Tenascin-C	TN-C
Volumetric Muscle Loss	VML

ABSTRACT

Author: Silva Garcia, Juan Martin. M.S.B.M.E.
Institution: Purdue University
Degree Received: August 2018
Title: Functionalization of Hyaluronic Acid Hydrogels with ECM-derived Peptides to Control Myoblast Behavior.
Major Professor: Sarah Calve

Volumetric muscle loss (VML) occurs when skeletal muscle injury is too large for the body's self-regenerative capabilities. As a consequence, fibrotic tissue fills the void, which reduces muscle functionality and limb movement. In the military, VML occurs mainly through explosions which represent more than 70% of total war injuries. Otherwise, the most common causes are traumatic accidents, tumor ablation, and musculoskeletal diseases.

Although a wide variety of natural and synthetic scaffolds have been studied with the purpose of providing the appropriate structural support, to date no scaffold has been able to significantly restore muscle functionality after VML. Satellite cells, adult stem cells within the muscle capable of self-renewal and restoring smaller injuries, are sensitive to the stiffness and composition of the surrounding environment. Scaffolds that only address structural support are not sufficient to restore muscle functionality and instead need to be designed to promote satellite cell activation as well. We hypothesized that generating a scaffold that mimicked the stiffness and composition of regenerating muscle tissue would promote good satellite cell recruitment into the scaffold.

One of the main extracellular matrix (ECM) molecules that is upregulated during scar-free repair is hyaluronic acid (HA). Therefore, thiol-modified HA and polyethylene glycol diacrylate (PEGDA) hydrogels were generated and functionalized with ECM-derived peptides that are highly upregulated during muscle regeneration, including RGD (found in fibronectin), IKVAV (found in laminin) or VFDNFVLK (found in Tenascin-C). Scaffolds with different stiffness were created by increasing the percentage of HA in the hydrogel. To test our hypothesis, we conducted an *in vitro* study quantifying the influence of HA stiffness and peptide functionalization on satellite cells and fibroblast cell proliferation, migration and gene expression. Results showed high promise for the use of HA hydrogels functionalized with the laminin peptide, IKVAV, due the promotion of cell spreading while enhancing cell migration, and the increase in gene expression of factors correlated with myogenic cell activation.

1. INTRODUCTION

1.1 Introduction / Background

In order to orchestrate muscle regeneration upon muscle injury, the extracellular matrix (ECM) undergoes remodeling, changing its composition and mechanical properties [1, 2]. The first changes to the composition of the ECM are upregulation of hyaluronic acid (HA), fibronectin and tenascins (TN). Fibronectin is thought to act as a framework to enable satellite cells, myogenic stem cells capable of self-renewal and muscle differentiation, to migrate into and within the muscle injury [3]. Meanwhile HA and TN-C upregulation has been correlated with the promotion of myogenic cell motility while preventing early differentiation [1]. Laminin upregulation also plays a substantial role during muscle regeneration by promoting satellite cell expansion and orchestrating their migration [4]. Once the wound has successfully been regenerated, laminin remains as one of the major components of the basal lamina where satellite cells reside [5]. Although the skeletal muscle regenerative response is highly effective, this process is dramatically hindered in severe injuries [6]. Large volume injuries, known as volumetric muscle loss (VML), are characterized by the loss of basal lamina, and the inability to regenerate [7, 8]. The basal lamina regulates the spatiotemporal events during muscle regeneration. It facilitates an ordered myofiber regeneration by properly guiding satellite cell activation and migration at the site of injury, where laminin plays a significant role [4, 9, 10]. Additionally, it delimits connective tissue from the functional myofiber to reduce scar tissue formation [9]. Although fibroblasts also play a role in the initial regenerative response, over proliferation accompanied with pro-fibrotic cytokine expression causes the infiltration of collagen I and collagen III at the site of injury [3, 11, 12]. The excessive fibroblast response, common in injuries where the basal lamina has been lost, disrupts the regenerative process and reduces muscle functionality and limb movement [13].

In the military, VML occurs mainly through explosions which represent more than 70% of total war injuries [14]. Otherwise, the most common causes are traumatic accidents, tumor ablation, and musculoskeletal diseases [8, 14]. Unfortunately for both civilians and military personnel, the current treatment consists of skeletal muscle transplantation, leading to harvest site morbidity [6, 15]. Although cell therapies have been investigated, the lack of ECM that supports a regenerative

response at the site of injury results in poor cell integration [16]. To this end, a wide variety of synthetic materials, natural materials, and even decellularized ECM-based scaffolds have been studied with the purpose of providing the appropriate structural support and orientation that embedded myogenic cells need for muscle regeneration [17]. Although some promising results have been reported, to date there has been no complete restoration of VML [17]. Hence, it is clear that a scaffold that provides structural support is insufficient. A scaffold that could provide not only structural support, but also facilitate the endogenous myogenic cell migration into, and proliferation within, the scaffold could help in enhancing body's regenerative response and restore the lost muscle.

HA is a non-sulfated glycosaminoglycan consisting of a repeating disaccharide unit consisting of α-1,4-D-glucuronic acid and β-1,3-N-acetyl-D-glucosamine[18]. During muscle regeneration, HA is highly upregulated and is thought to promote cell migration, proliferation, and maintenance of stem cell phenotype [18]. HA is a popular scaffolding material for regeneration purposes among different tissues since it is biocompatible, facilitates diffusion of nutrients, and regulates tissue hydration [19]. Fabrication of HA-based scaffolds has been achieved through different chemical modifications usually targeting the carboxyl and hydroxyl groups of the disaccharide [19]. One modification method includes conjugation of dithiobis(propanoicdihydrazide) onto carboxylic acid moieties present in glucuronic acid of HA to produce thiolated HA , using carbodiimide chemistry [20]. After reducing disulfide bonds, free thiols enable crosslinking of HA chains through a Michael type addition reaction with acrylates present in the biological inert polymer, polyethylene glycol diacrylate (PEGDA). The PEG allows to control pore size, and the thiol-acrylate reaction (Michael-type addition) is fast and ensures biocompatibility by occurring at a physiological pH and temperature [21], making it suitable for an *in situ* cross-linkable scaffold [21]. However, HA supports little cell attachment due in part to its high electronegativity [22, 23]. To overcome cell attachment limitation peptides that support cell adhesion can be grafted into scaffolds. Although a fibronectin peptide, RGD, has been used in numerous biomaterial systems to promote cell adhesion [24], we wanted to investigate whether other ECM-derived peptides could better promote cell attachment of myogenic cells over connective tissue cells. Equally as important, peptide ligand recognition by distinct integrins stimulates numerous and different signaling pathways that affect motility, proliferation and differentiation of myogenic and connective tissue

cells; influencing the balance between fibroblasts and satellite cells which is thought to impact the formation of either fibrotic or regenerated tissue [25]. Thus, by examining different peptides, we anticipated that we could tailor the scaffold environment to maximally support muscle regeneration.

With the goal of engineering a scaffold that could increase the number of satellite cells over fibroblasts to promote VML repair, in this study, thiol-modified HA and PEGDA hydrogels were functionalized with ECM-derived peptides, including, RGD (found in fibronectin), IKVAV (found in laminin) or VFDNFVLK (found in tenascin-C (TN-C)). Scaffolds with storage moduli (G') ranging from to 400 Pa to 2 kPa were developed by increasing HA content of the hydrogel, and the *in vitro* effect of peptide type and hydrogel stiffness on myogenic and fibroblast cells behavior was quantified.

2. MATERIALS AND METHODS

Unless otherwise specified, all reagents were of cell culture grade from Thermo Fisher.

2.1 HA-DTPH synthesis

DTPH-modified HA was synthesized as described [26]. Briefly, 100 kDa sodium hyaluronate (Lifecore Biomedical) was dissolved at 10 mg/mL in degassed Milli-Q water. Dithiobis(propanoicdihydrazide) (DTP; Frontier Scientific) was added at a molar ratio of 1 HA: 2 DTP while stirring. DTP was incorporated by activating the carboxyl group of β-D glucuronic acid of HA using (1-ethyl-3-(3-dimethylaminopropyl) carbodiimide (EDC) at a pH of 4.75. The reaction was stopped after 1 h by increasing the pH to 7 with the addition of 1 M sodium hydroxide (NaOH) so that 26% of the available glucoronate carboxyl groups were functionalized with a disulfide bond present in DTP.

Next, the disulfide bond of DTP was reduced using dithiothreitol (DTT) at a molar ratio of 1 DTP: 5 DTT at a pH of 8.5 for 24 h while stirring. The hyaluronic acid-dithiobis(propanoichydrazide) (HA-DTPH) solution was then transferred to a dialysis membrane (15 kDa cut-off) and dialyzed against a 0.3 mM hydrogen chloride (HCl) solution (pH 3.5) with 100 mM sodium chloride (NaCl), and the dialysis solution was replaced daily for 2 weeks. This was followed by dialysis against 0.3 mM HCl solution (pH 3.5) without NaCl, dialysis solution was replaced daily for 1 week. HA-DTPH solution was frozen at -80 °C, lyophilized and kept at -80 °C for long-term storage and -20 °C for a storage duration less than 2 weeks. The resulting free thiol content was measured using Ellman's method [27, 28]. The number of thiols per 100 disaccharide units of HA was calculated by dividing thiol molar concentration by non-thiolated HA molecular weight.

2.2 Hydrogel preparation

2.2.1 Peptide-PEGDA solutions

Stock concentration of peptide-free poly (ethylene glycol) diacrylate (PEGDA) at 1.78%, 3.56%, and 5.34% (w/v) were prepared in advanced DMEM (high glucose with sodium pyruvate, cat# 12491015). Except for IKVAV, 4 mM peptide stock solutions were made in Milli-Q water. 4 mM

IKVAV stock solution was prepared in 20% acetic acid and adjusted to pH 8 by first dissolving IKVAV in 20% acetic acid (10% of final volume), then adding 10x PBS (10% of final volume). The pH was adjusted to 8 with 1 M NaOH and volume was adjusted with 1x PBS. Both PEGDA and Peptide stock solutions were sterilized by filtration through a 0.22 µm syringe filter before use. Next, PEGDA was functionalized with one of the peptides listed in Table 1 to generate peptide-PEGDA. Peptide functionalization was performed via Michael-type addition between the terminal cysteine on the peptide (Table 1) and one acrylate group on PEGDA at pH 7.4 for 40 min at 37 °C in a humidified 5% CO_2 incubator. Each stock solution was made at a working concentration of 294 µM, 558 µM, and 1,176 µM.

Table 1. ECM-derived peptides used in the study

	Peptide sequence	Reference
Fibronectin	Cys-Gly-Arg-Gly-Asp-Ser (CGRGDS)	[29, 30]
Tenascin- C	Val-Phe-Asp-Asn-Phe-Val-Leu-Lys-Gly-Ser-Cys (VFDNFVLKGSC)	[31]
Laminin	Cys-Ser-Gly-Ile-Lys-Val-Ala-Val (CSGIKVAV)	[32]

2.2.2 HA-DTPH solutions

HA-DTPH solutions were prepared by dissolving lyophilized HA-DTPH in advanced DMEM and the pH was adjusted to 7.4 by adding 1.0 M NaOH, yielding HA-DTPH working stock solutions of 2%, 4%, 6% (w/v). Each stock solution was sterilized by filtration through a 0.22 µm syringe filter.

2.2.3 Hydrogel preparation

Hydrogels were formed by crosslinking the electrophilic acrylate groups of PEGDA with the reduced thiols of the HA via Michael-type addition. Peptide-free PEGDA and peptide-PEGDA was added to HA-DTPH at a ratio of 1:1 and then mixed for 15 s to generate 1%, 2%, and 3% (w/v) HA hydrogels and a peptide end concentration of 0 µM, 147 µM, 294 µM, 588 µM. The final HA-DTPH/PEGDA ratio (w/w) was 1.12. HA-DTPH/PEGDA solutions were quickly

pipetted into a µ-slide angiogenesis slide (ibidi;10 µl per well for cell culture), 48 well plate (150 µl per well for gene expression analysis) or Teflon covered slide (200 µl for rheological testing) and incubated for 1 h (cell culture), and 5 h (gene expression and rheological testing) at 37 °C in a humidified 5% CO_2 incubator. After gelation, HA hydrogels were swelled under the same incubation conditions for 15 h with the addition of advanced DMEM supplemented with 1% fetal bovine serum (FBS, Atlanta Biologicals), 1% L-Glutagro (Corning), and 1% Penicillin-Streptomycin before cell-based or rheology assays.

2.3 Rheological characterization

The viscoelastic mechanical properties of the hydrogels were measured with an AR2000 rheometer (TA) using a parallel plate geometry with a 20 mm diameter at a starting normal force of 1 N. The hydrogels were prepared, incubated and swelled as previously stated above. The linear range of the viscoelastic response was first measured with an angular frequency sweep ranging from 0.1 to 200 rad/s at 0.5% strain. The storage and loss moduli of the hydrogels were measured with an increasing oscillatory stress sweep from 0.1 Pa to 100 Pa at 1 rad/sec. Teflon slides were secured to the bottom plate with tape to prevent movement during the test.

2.4 Cryo-SEM

Differences in pore diameter between 1%, 2%, and 3% (w/v) HA hydrogels were visualized by cryo-scanning electron microscopy (Cryo-SEM). Cryo-SEM was performed on a FEI NovaNanoSEM with a GATAN Alto 2500 cryo-system. HA-DTPH/PEGDA solutions were pipetted into a SEM stub adaptor and incubated for 1 h at 37 °C in a humidified 5% CO_2 incubator before swelling for 15 h. Individual samples were flash-frozen by immersion in liquid nitrogen and then fractured with a scalpel. Fractured samples were then lyophilized inside the cryo-system and sputtered with platinum. Images were taken at 5 kV with a spot size of 3 and 10,000× magnification. Pore diameter was calculated by measuring the length of a draw line between two opposite points of the pore using FIJI (NIH).

2.5 In-vitro cell expansion and cell culture

2.5.1 Primary isolation and cell culture

Murine experiments were approved by the Purdue Animal Care and Use Committee (PACUC; protocol #1209000723). PACUC ensures that all animal programs, procedures, and facilities at Purdue University adhere to the policies, recommendations, guidelines, and regulations of the USDA and the United States Public Health Service in accordance with the Animal Welfare Act and Purdue's Animal Welfare Assurance. Pax3-Cre [33] and ROSA-ZsGreen1 transgenic mice [34] were obtained from the Jackson Laboratory (Bar Harbor, ME, USA) and used to generate Pax3-Cre/ZsGreen1+ progeny in which the satellite cells are GFP+.

Tibialis anterior (TA) muscles were harvested from 3-4 week old mice. Each pair of TAs were placed in a digestion solution consisting of advanced DMEM and 2 mg/ml collagenase type II (Worthington Biochemical). After incubation for 1-1.5 h in a shaking water bath at 37 °C, the suspension was passed through a 70 μm strainer to remove debris and undigested tissue. To completely remove all collagenase type II, the cell suspension was centrifuged, supernatant aspirated and resuspended in growth medium [DMEM (high glucose with sodium pyruvate, cat#10313), supplemented with 10% FBS, 1% L-Glutagro, and 1% Penicillin-Streptomycin], two times. Cells were then plated in a 100 mm dish (Greiner CELLSTAR) and cultured in growth medium at 37 °C in a humidified 5% CO_2 incubator.

The resulting cell population was composed of GFP+ myoblasts and GFP- cells, the latter of which were predominantly fibroblasts. The heterogeneous population of cells was expanded until 80% confluent and then passaged by dissociating cell monolayers with 1.5 mL trypsin/EDTA, centrifuged, resuspended in growth medium and replated at 1:2. Cells were expanded and passaged 3 times before separating GFP+ from GFP- cells by fluorescence-activated cell sorting (FACS) using a FACSAria III flow cytometer. GFP+ cells were cultured in growth medium with 4 ng/ml recombinant murine FGF-2 (PeproTech) at 37 °C in a humidified 5% CO_2 incubator. GFP- cells were cultured in growth medium at 37 °C in a humidified 5% CO_2 incubator. Cell subpopulations were expanded until 80-90% confluent and then passaged by dissociating cell monolayers with 1.5 mL trypsin/EDTA, centrifuged, and resuspended in growth medium and replated at 1:2. Cells were expanded and passaged a maximum of 4-5 times prior to any experiment.

Trypsinization can cause proteolytic breakdown of functional integrins on the cell membrane [35], causing a detriment to cell and ECM-derived peptide interaction. Therefore, before any cell-based experiment, cell monolayers were dissociated with 10mM EDTA in Milli-Q water with an adjusted pH of 7.4, centrifuge, and resuspended in supplemented advanced media.

2.5.2 Cell migration

Each cell subpopulation was seeded on the surface of 1%, 2% or 3% (w/v) HA hydrogels previously formed in a µ-slide angiogenesis slide, at a density of 5,000 cells/cm^2. Cells were allowed to attach and equilibrate at 37 °C in a 5% CO_2 on a Leica DMI600 fluorescent microscope equipped with a PECON BLX Black Incubator for 3 h, followed by time-lapse imaging with a frequency of 1 image per hour for 24 h, at 5x. Individual cell migration was quantified over the first 12 h using the Manual Tracking plugin in FIJI.

2.5.3 Cell proliferation

Cells were plated on 1% 2% or 3% (w/v) HA hydrogels as described above at a density of 5,000 cells/cm^2. Cells were cultured for 3 h at 37 °C in a humidified 5% CO_2 incubator. Half of the media of each well was then carefully pipetted out. Then, 1 mM of 5-ethynyl-2'-deoxyuridine (EdU) in 1x PBS was diluted in growth medium to a concentration of 2 µM, and added to each well (final concentration of EdU = 1 µM). Cells were cultured for 24 h and then fixed in 4% paraformaldehyde (Sigma) for 20 min, rinsed in PBS, permeabilized with 0.5% Triton X-100 (Amersham Life Science) in PBS for 10 min and then rinsed in PBS. Cells were blocked for 15 min [blocking buffer: 20% goat serum, 0.2% bovine serum albumin (Sigma)], rinsed in PBS, stained with 5 µM AF555 picolyl-azide toolkit following manufacturer's instructions, and with 1:500 DAPI of 1 mM in PBS for 10 min. The entire well was imaged with a tile scan at 5x using a Leica DMI600 fluorescent microscope, and the number of cells actively synthesizing DNA was quantified by dividing the number of nuclei with EdU incorporation by the total number of nuclei visualized with DAPI.

2.6 Gene expression analysis

Cells were seeded on the surface of 1%, 2% or 3% (w/v) HA hydrogels on a 48-well plate at a density of 5,000 cells/cm^2. RNA was isolated according to manufacturer's instructions using a

Qiagen miRNA kit. Total RNA was converted to cDNA using iScript cDNA synthesis kit (BIO-RAD) in a thermal cycler (BIO-RAD). Quantitative PCR (qPCR) was performed using SsoAdvanced Universal SYBR Green Supermix (BIO-RAD) with a real-time PCR detection system CFX96 (BIO-RAD). Changes in relative expression for the genes of interest were calculated using GAPDH as reference gene. Primer sequences for target genes are listed in Table 2.

Table 2. Primer sequences for qPCR analysis.

Gene	Forward Primer 5′-3′	Reverse Primer 5′-3′	Size, bp	Ref Seq
Pax7	GAATCAGAACCCGACCTCCC	CGCCGGTTACTGAACCAGA	191	NM_011039.2
MyoD	GAACCCAACCTGAACGTCTG	GTGTGGCCGCCATTCTTTATC	91	NM_010783.3
MyoG	GCAGGCTCAAGAAAGTGAATGA	TAGGCGCTCAATGTACTGGAT	122	NM_001164048.1
MyF5	AAGGCTCCTGTATCCCCTCAC	TGACCTTCTTCAGGCGTCTAC	249	NM_008656.5
GAPDH	TGGAAAGCTGTGGCGTGAT	TGCTTCACCACCTTCTTGAT	216	NM_008084.2

2.7 Statistical analysis

Results are presented as mean ± standard deviation (SD). Statistical analysis was performed using Graphpad Prism 7 (La Jolla, Ca).

Two-way ANOVA and Tukey's post hoc test were used to assess the effect of peptide and %HA on storage modulus, cell migration, DNA synthesis, and gene expression. One-way ANOVA and Tukey's post hoc tests were used to assess differences in pore size across the different %HA hydrogels. In general, the sample size consisted of three independent experiments with at least three technical replicates each. Statistical significance was considered at a value of $\alpha<0.05$. Statistical significance is represented as follows: $*p<0.05$, $**p<0.01$, $***p<0.001$.

3. RESULTS

3.1 Characterization of peptide-functionalized hydrogels

To examine how the mechanical properties of hydrogels were influenced by HA concentration and peptide addition, gels were tested with a rheometer. The linear viscoelastic range was determined from angular frequency sweeps (0.1-200 rad/sec) of the HA-DTPH PEGDA hydrogels. A 0.5% strain applied to the hydrogels produced constant storage modulus (G') values indicating that the samples were independent of the applied angular frequency (up to 10 rad/sec). Therefore, an angular frequency of 1 rad/sec was used to determine G' by testing hydrogels with an oscillatory stress sweep ranging from 0.1 – 100 Pa (Fig. 1). G' was compared between samples at an oscillatory stress of 10 Pa. As expected, G' significantly increased as HA concentration increased from 1% to 3% (w/v) ($p < 0.05$; Fig. 1). Notably, G' was much higher than the loss modulus (G''), demonstrating that the rheological response is mainly dominated by elastic behavior (Fig. 2).

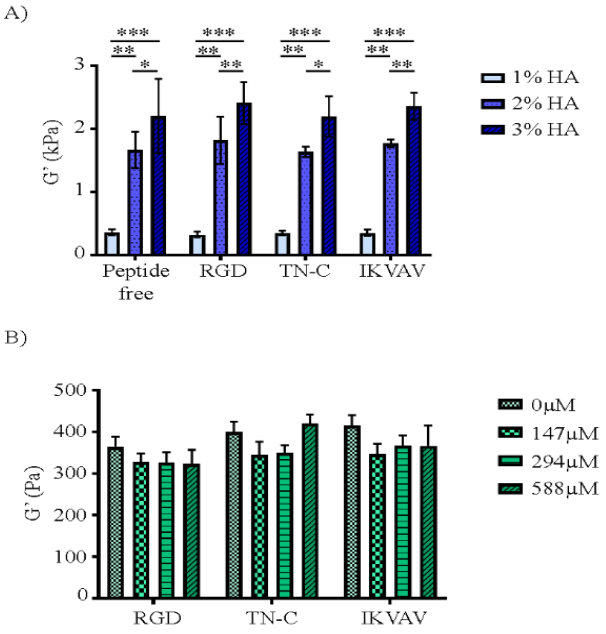

Figure 1. Storage modulus of HA hydrogels is not affected by peptide functionalization. (A) G' significantly increased as HA concentration increased from 1 – 3 % (w/v). Oscillatory shear stress was performed at 1 rad/sec and G' determined at an oscillatory shear stress of 10 Pa. Two-way ANOVA indicated that HA percentage significantly affected G' (p<0.05), whereas functionalization with 294 μM peptide did not. Tukey's post-hoc test revealed significant differences between G' of different gel percentages (*p<0.05, **p<0.01, ***p<0.001). (B) Functionalization of 1% HA with 0 - 588 μM peptide did not significantly affect G'. Error bars = SD, n = 4 for each treatment.

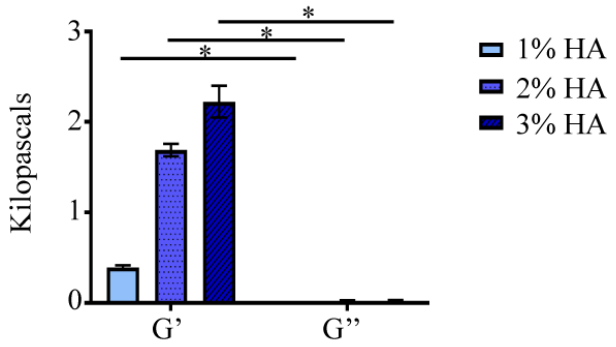

Figure 2. Rheological response of HA hydrogels is dominated by elastic behavior. Oscillatory shear stress was performed at 1 rad/sec and G', G'' determined at an oscillatory shear stress of 10 Pa. Two-way ANOVA indicated that G' is statistically higher than G'' (p<0.0001). Tukey's post-hoc test revealed significant differences between G' and G'' of the same HA hydrogel percentages (p<0.0001). Error bars = SD, n = 4 for each treatment.

To assess if peptide addition had an impact on mechanical properties, the hydrogels were functionalized with up to 588 µM peptide, double the concentration used in subsequent studies. Results showed that G' was not significantly affected by peptide functionalization (Fig. 1). To study the inner structure of the hydrogel, images of the pore structure were resolved by Cryo-SEM. For the three %HA hydrogels a honeycomb pore structure was revealed. Further quantification showed inner pore diameter was significantly smaller in the 3% HA hydrogels (p < 0.001; Fig. 3).

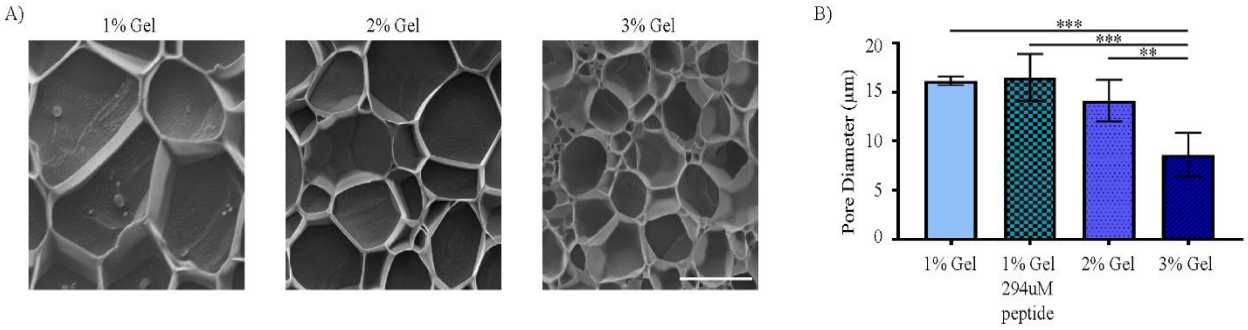

Figure 3. Pore diameter of hydrogels decreases as HA percentage increases. (A) Representative Cryo-SEM images for 1 – 3% HA hydrogels. Bar = 10 µm (B) One-way ANOVA indicated that pore diameter was significantly affected by HA% (p<0.001). Tukey's post-hoc test revealed a significant decrease in pore diameter in the 3% HA hydrogel compared to the other hydrogels. (**p<0.01, ***p<0.001). Peptide functionalization did not significantly affect pore diameter. Error bars = SD, n=4 for each treatment.

3.2 Peptide type and %HA have a profound effect on GFP+ and GFP- cell proliferation

Fibrotic tissue formation is thought to be caused by high expansion of connective tissue cells compared to preferential activation of satellite cells at the site of injury [11]. Therefore, we determined the influence of %HA and different ECM-derived peptides on cell proliferation by quantifying the number of cells that were actively synthesizing DNA. In order to separately analyze the effect of %HA and peptide type on the behavior of muscle progenitors and the surrounding connective tissue cells, we used a mouse model in which muscle progenitors were labeled with GFP. Muscle-derived cells were isolated from the tibialis anterior muscle of Pax3-Cre/ZsGreen1 mice and sorted using FACS to generate GFP+ (satellite cells) and GFP- (connective tissue) cells. Unless specified, data was normalized to the 1% HA peptide-free hydrogels.

Overall, the HA hydrogels stimulated higher DNA synthesis of GFP+ cells compared to the GFP- cells (Appendix Fig. 1). Variations in %HA in the peptide-free hydrogels did not have a significant impact on DNA synthesis of GFP- cells (Fig. 4). However, when 3% HA hydrogels were functionalized with either peptide, a significant increase on DNA synthesis was observed in comparison with the other percentages ($p < 0.05$). To note, both GFP+ cells and GFP- cells increased in cell proliferation on the 2% HA hydrogels.

Taken together, DNA synthesis by GFP- cells is upregulated regardless of the peptide type used in this study, as long as higher %HA hydrogels are used. Meanwhile, DNA synthesis of GFP+ cells was specifically stimulated on the 2% HA hydrogel functionalized with RGD ($p < 0.05$).

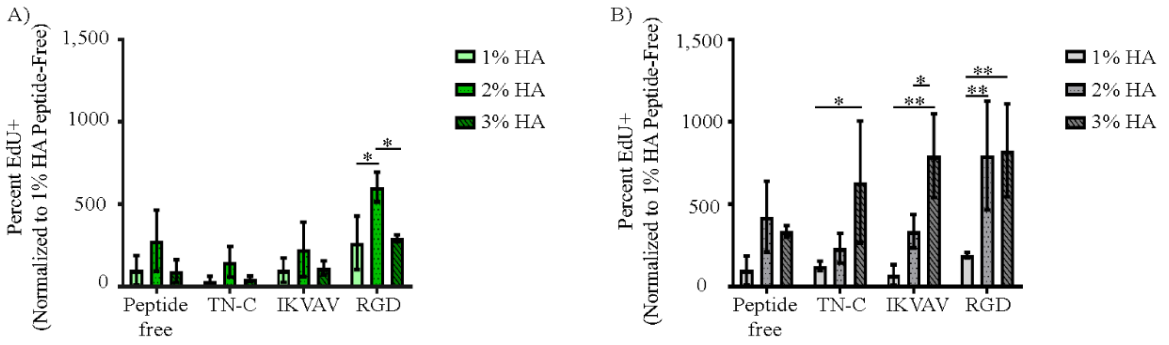

Figure 4. DNA synthesis by GFP+ and GFP- cells is influenced by %HA and type of peptide. Overall DNA synthesis by GFP+ cells was greater than that by the GFP- cells (Appendix Fig. 9). A) GFP+ cells showed the highest DNA synthesis on the 2% HA hydrogels functionalized with RGD. Two-way ANOVA revealed significance for peptide ($p<0.05$) and gel percentage ($p<0.0001$). B) Two-way ANOVA revealed significance for peptide ($p<0.05$) and gel percentage ($p<0.0001$) on GFP- cell migration. Tukey's post hoc tests showed a significant increase in DNA synthesis on the 3% peptide-functionalized hydrogels. GFP+ and GFP- cells were cultured *in vitro* for 24 h and the percentage of cells that synthesized new DNA was determined by labeling for EdU incorporation (*$p<0.05$; **$p<0.005$). Error bars = SD; $n \geq 360$ cells per hydrogel combination.

3.3 Peptide type and %HA affects cell migration

In addition to proliferation, satellite cell migration to the site of injury is critical for the promotion of muscle repair. Therefore, we determined the influence of %HA and ECM-derived peptides on the migration of FACS isolated GFP+ and GFP- cells. Overall, the addition of RGD significantly decreased cell migration of both GFP+ and GFP- cells compared to the other hydrogels (Fig. 5). Additionally, the combination of RGD with the increase in %HA further reduced cell migration, GFP+ cells ($p < 0.001$).

Promotion of cell migration by TN-C incorporation was observed only in the 1% HA hydrogel and only for GFP+ cells. Interestingly, the combination of %HA and IKVAV incorporation had opposite effect on the migratory response of the two cell types. While the increase in %HA accompanied with IKVAV incorporation enhanced GFP+ cell migration ($p < 0.001$), a reduction on GFP- cell migration was observed ($p < 0.05$).

Taken together, GFP+ cell migration showed more sensitivity to changes in %HA and type of peptide, whereas GFP- cell migration was mainly affected by type of peptide. The latter can be confirmed by noting no difference in GFP- cell migration on peptide-free hydrogels, while GFP+ migratory response was significantly affected by %HA within each peptide group.

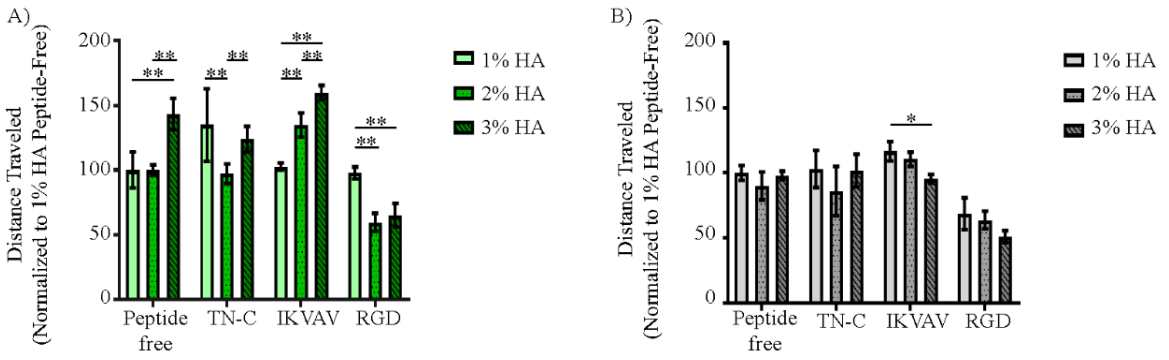

Figure 5. Migratory response of GFP+ and GFP- cells is influenced by %HA and type of peptide. There was an overall decrease in GFP+ and GFP- cell migration on RGD-functionalized hydrogels. While TN-C-functionalized hydrogels had a similar effect on both GFP+ and GFP- cells, IKVAV-functionalized hydrogels had an opposite effect on the migratory response of the two cell types. A) GFP+ cells migratory response was significantly affected by %HA within each peptide group. Two-way ANOVA showed significance for peptide/%HA interaction ($p<0.0001$), peptide ($p<0.0001$), and %HA ($P<0.0001$). Tukey's post hoc test revealed the effect of %HA on the different peptide groups (*$p<0.05$, **$p<0.01$, ***$p<0.001$). B) Total distance traveled by GFP- cells was of a similar magnitude as GFP+ cells (Appendix Fig. 10); however, the migratory response was less affected by %HA. Two-way ANOVA showed significance for %HA ($p<0.05$) and type of peptide ($p<0.0001$). Tukey's post hoc test revealed difference in cell migration by IKVAV-functionalized hydrogels between 1% and 3% HA (*$p < 0.05$). GFP+ and GFP- cells were imaged and tracked every hour for 12 h. Error bars = SD; $n \geq 100$ cells per %HA-peptide combination.

3.4 Hydrogel mechanical properties along with RGD and IKVAV incorporation enhanced cell spreading

Due to the electronegativity of hyaluronic acid coupled with the potential lace of hyaladherins on the cells, cells are unable to attach properly to the peptide-free hydrogel. Cell attachment and cell spreading correlates with increased cell viability and proliferation [36]. Therefore, promotion of cell attachment and spreading by ECM-derived peptides on GFP+ and GFP- cells on the hydrogels was assessed after 24 h.

Overall, GFP+ and GFP- cells spread more on the HA hydrogels functionalized with RGD and IKVAV in comparison to TN-C and peptide-free hydrogels. Interestingly, cluster formation seen on the peptide-free hydrogels was diminished on the 2% HA hydrogels for both GFP+ and GFP- cells (Fig. 6-7), and then diminished on the 3% HA hydrogels. The latter demonstrates the importance of hydrogel mechanical properties in regulating cell attachment and cell spreading.

As seen on the peptide-free hydrogels, differences in cell spreading and intercellular binding were seen across the different %HA hydrogels functionalized with either RGD or IKVAV. Of note, for

GFP+ cells, both 2% and 3% HA hydrogels enhanced cell spreading in a similar way among hydrogels with RGD or IKVAV incorporation. However, GFP- cells were more susceptible to changes in %HA. As shown in Fig.7. IKVAV promoted higher cell spreading on the 2% HA hydrogels while RGD incorporation enhanced cell spreading on the 3% HA hydrogels.

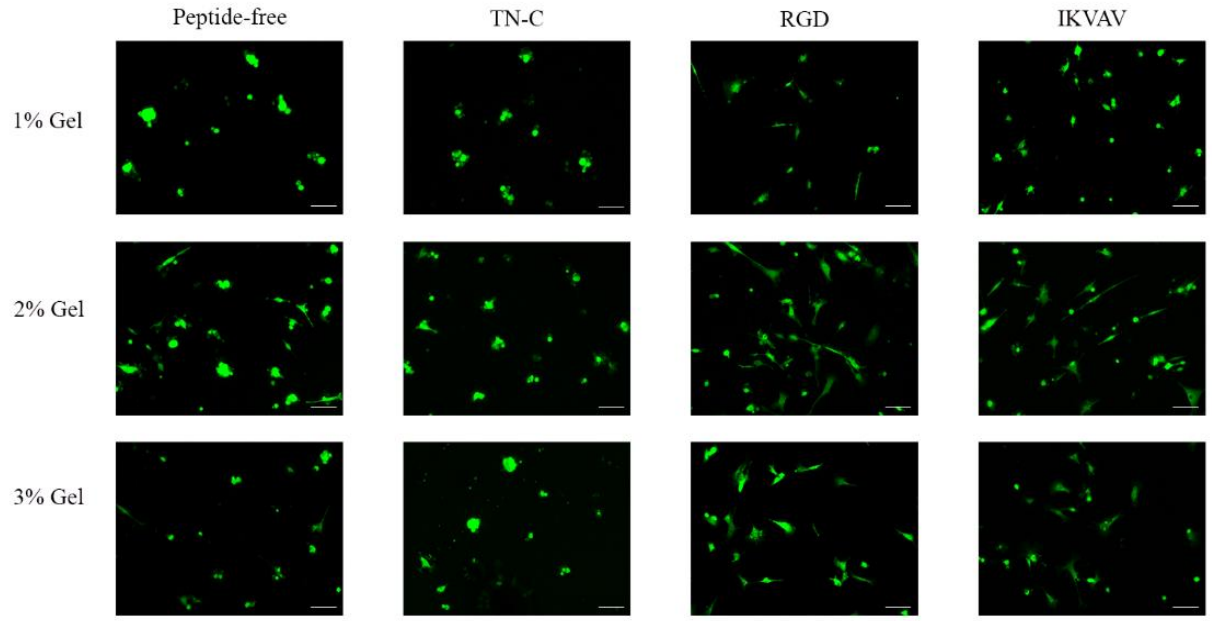

Figure 6. Incorporation of ECM-derived peptides and hydrogel stiffness impacts the attachment and spreading of GFP+ cells. RGD and IKVAV-functionalized hydrogels enhanced cell spreading in comparison to the cell clustering effect observed on peptide free and TN-C-functionalized hydrogels. Interestingly, hydrogel stiffness caused evident differences in cell phenotype within each hydrogel group. Bar = 100 µm.

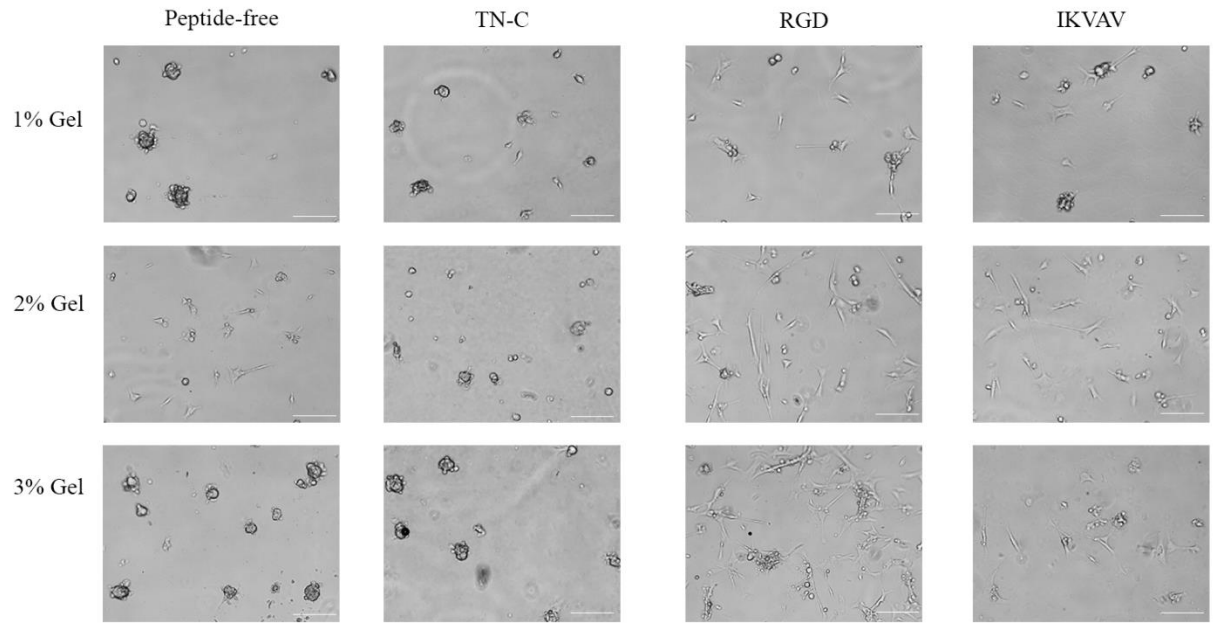

Figure 7. Incorporation of ECM-derived peptides and hydrogel stiffness impacts the attachment and spreading of GFP- cells. Similar to GFP+ cells, RGD and IKVAV-functionalized hydrogels promoted higher cell attachment and cell spreading. Cell spreading was enhanced on RGD-functionalized hydrogels as gel percentage increased. In comparison, the IKVAV-functionalized hydrogels promoted higher cell spreading on the 2% HA hydrogel. Bar = 100 μm.

3.5 MyoD and Pax7 are significantly upregulated by IKVAV on the 3% HA hydrogels

In mature muscle, satellite cells reside in a quiescent form until they are activated in response to extrinsic signals such as changes in ECM during muscle repair [37]. Once activated, satellite cells proliferate, and progeny fuse with damaged myotubes or with each other to form differentiated myotubes [6]. Activation, proliferation, and differentiation of satellite cells is regulated by changes in expression of myogenic regulatory factors (MRFs), including MyoD, Myf5 and MyoG [37]. Paired box protein (Pax7) a transcription factor express in satellite cells has gained attention, since expression has been correlated with satellite cell self-renewal [38].

Therefore, we analyzed how expression of Pax7 and the myogenic factors involve in satellite cell activation [MyoD], self-renewal [Myf5], and differentiation [MyoG] were affected by %HA and type of peptide on GFP+ cells. Gene expression was assessed at 24 h post cell seeding.

Surprisingly, significant differences were found only in MyoD and Pax7 gene expression. Both MyoD and Pax7 were significantly upregulated on the 3% HA hydrogel peptide-free and 3% HA hydrogel functionalized with IKVAV (Fig. 8).

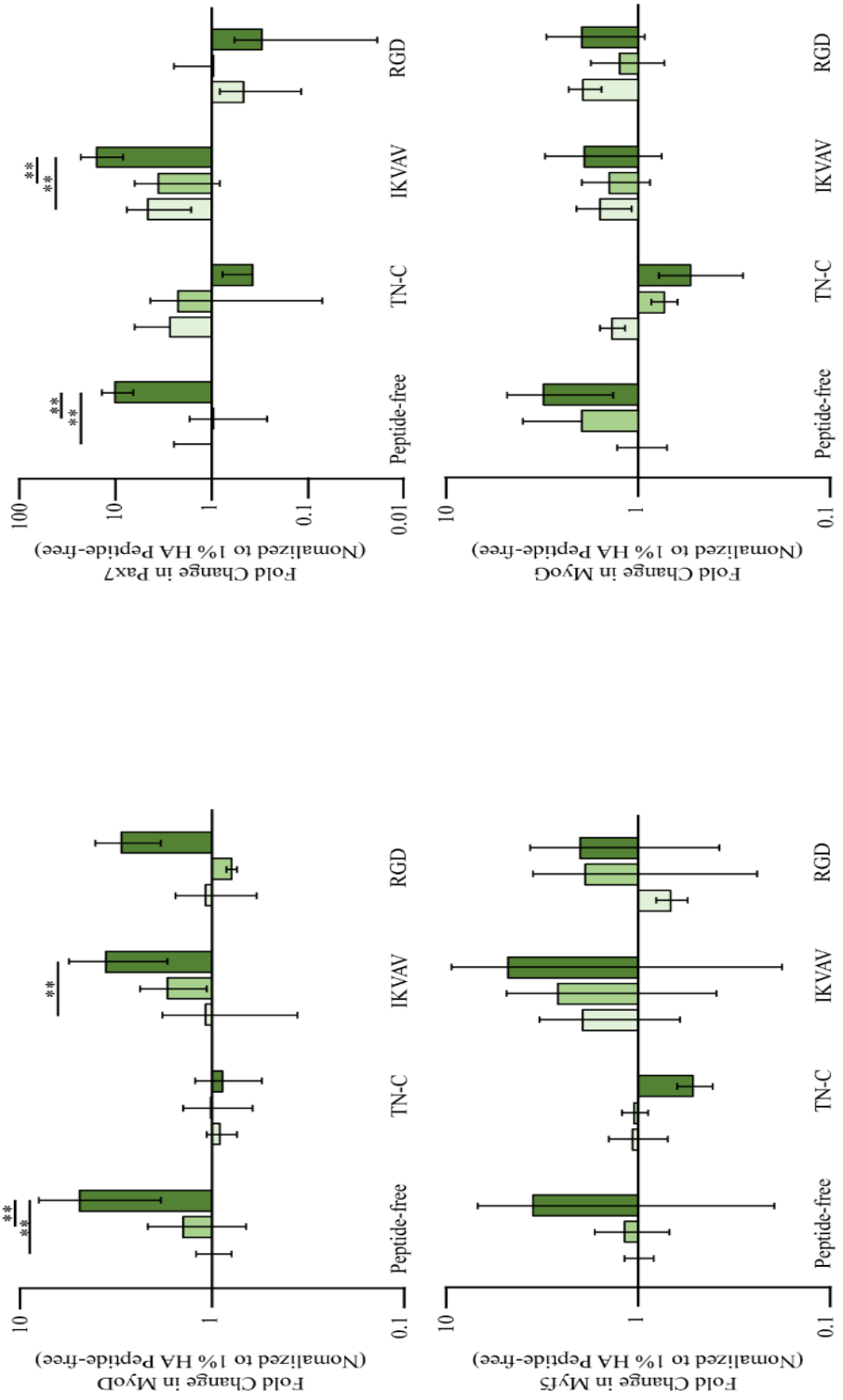

Figure 8. MyoD and Pax7 expression was highly upregulation on the 3% HA hydrogels functionalized with IKVAV and peptide-free. MyoD Two-way ANOVA showed significance for %HA (p<0.01). Pax7 Two-way ANOVA showed significance for %HA (p<0.01) and type of peptide (p<0.01). Tukey's post hoc test revealed the effect of %HA on the peptide-free and IKVAV functionalized hydrogels for MyoD and Pax7 (*p<0.05; **p<0.005). Error bars = SD; n = 3.

4. DISCUSSION

Providing the necessary framework to sustain cell migration, viability, and proliferation is necessary to promote muscle regeneration after VML. Even though fibroblast synthesis of ECM is an important step for muscle regeneration, a regulated expansion of this cells and the enrichment of satellite cells at the site of injury is needed to avoid fibrotic tissue formation [3, 17].

In this study, we analyzed the influence of ECM-derived peptides and stiffness on myogenic and connective tissue cell behavior. By varying the HA content in the gel three distinct types of oscillatory stiffness were acquired by increasing %HA. The 1,2,3 %HA hydrogels had a storage modulus (G') of 400 Pa, 1.7 kPa and 2 kPa respectively.

HA upregulation has been correlated with numerous cell responses, from promoting cell proliferation to stimulation of cell motility, depending on its molecular weight and the type of cell interacting with the HA [19, 39]. In our studies, the low molecular weight HA (100 kDa) used in our HA based hydrogels, promoted higher proliferation of satellite cells in comparison with connective tissue cells (Appendix Fig. 1). The latter correlates with past studies showing that HA upregulation enhances stem cell proliferation [19].

Fibronectin is one of the first ECM proteins that is upregulated upon muscle injury. It is thought that fibronectin is secreted with the purpose of providing a support framework after injury, enabling satellite cell proliferation at the site of injury [40]. To this end we incorporated RGD, a well-known sequence present in fibronectin. Interestingly, RGD significantly enhanced cell proliferation on the 2% HA hydrogels with G' of 1.7kPa. Correlated with past studies showing that changes in stiffness controls satellite cell fate [2, 13], the down regulation of DNA synthesis on the 3% HA hydrogels functionalized with RGD could be caused by the induction of satellite cell differentiation on substrates with higher stiffness [13]. Similarly, RGD was able to stimulate a higher DNA synthesis on the 2% HA hydrogels for GFP- cells. However, in contrast with GFP+ cells, DNA synthesis stimulation remained on the 3% HA hydrogels functionalized with RGD for GFP- cells. Functionalization of the 3% HA hydrogels stimulated DNA synthesis regardless of the ECM-based peptide used in this study. The latter not only correlates with previous studies in which increasing stiffness of scaffolds correlated with greater fibroblast proliferation [41], but could also indicate that stiffness contributes to connective tissue cell over proliferation at the site of injury compared to myogenic cell proliferation [11].

TN-C is a matricellular protein highly upregulated during the wound healing process [1]. Upregulation of TN-C has been correlated with myoblast cell motility [42]. Similarly, a TN-C peptide, VFDNFVLK, has been correlated with stimulation of cell migration of neurites through the α7β1 integrin [31]. The α7β1 integrin is an integrin highly expressed in myogenic cells [43]. Therefore, we expected the stimulation on GFP+ cell migration, which interestingly varies with gel stiffness. However, while GFP+ cells were observed in increase migration at the highest HA concentration, the TN-C peptide exhibited a u-shaped curve, suggesting that satellite cells respond differently to stiffness depending on the ECM cues made available.

Stiffness effect on GFP+ cell migration correlates with previous studies demonstrating that substrate stiffness affects myogenic cell migration [44]. As for %HA having no effect on GFP- cell migration; Ghosh et al, quantified fibroblasts cell migration on an HA hydrogel with a G' of 4.2 kPa [45]. Interestingly, GFP- cells seeded in our 2 kPa (3% HA hydrogel) migrated at a similar rate as the fibroblasts seeded on the 4.2 kPa. Demonstrating that fibroblast cell migration is not as susceptible to changes in G' between 400 Pa (1% HA hydrogel) and 4.2 kPa as GFP+ cells.

Consistent with past reports showing that HA polyanionic properties decrease cell adhesion [22, 23], both cell types seeded on the peptide-free hydrogel maintained a clumped phenotype, indicating the need for peptide functionalization for enhanced cell-gel interactions and focal adhesion formation. Additionally, HA and TN-C upregulation have been correlated with stimulation of myoblast cell motility while inhibiting cell differentiation [1]. The latter could be the reason why peptide-free and TN-C-functionalized HA hydrogels promoted cell locomotion while inhibiting cell spreading on both cell types. Cell spreading was promoted with the incorporation of RGD or IKVAV peptide on both cell types. Differences in cell spreading were observed across different %HA, highlighting the importance of external mechanical stimuli exerted on cells by the surrounding matrix. Increased cell spreading, and cell junctions were noticeable on HA hydrogels functionalized with RGD, especially on the stiffer substrate, 3% hydrogel, for GFP- cells (Fig. 7). The latter agrees with findings demonstrating that fibronectin highly promotes connective tissue cell adhesion and spreading [46]. HA hydrogels functionalized with either RGD or IKVAV promoted cell spreading at a similar degree on GFP+ cells (Fig. 6). However, fibronectin has been correlated with rapid vinculin focal contact formation accompanied with organized α-actinin [47] causing strong focal contact formation. The latter could represent the cause of why GFP+ and GFP- cells seeded on RGD had the lowest cell migration in our studies. In contrast laminin promotes diffuse vinculin and α-actinin [47], which could be why IKVAV incorporation enhanced cell spreading while maintaining a locomotory advantage over RGD. Most likely IKVAV cell motility enhancement was promoted through the interaction between ligand and the α3β1, α6β1, and α6β4 integrins [32, 48, 49] for GFP+ cells while for GFP- mainly through α3β1 integrins [50].

Quiescent satellite cells express the transcription factor Pax7. Upon injury, satellite cells are activated, transitioning from a cell cycle arrest, G0 phase, to a G2 phase where mitosis is followed [37]. Activated satellite cells express both MyoD and Pax7 [38]. In our studies both genes were significantly upregulated on the 3% HA hydrogels that were peptide-free or functionalized with IKVAV. Interestingly, both peptide-free and IKVAV incorporation on the 3% HA hydrogels showed the highest cell migration of GFP+ cells. Pax7 upregulation has been correlated with myogenic cell migration for a successful limb formation during development [51]. Further correlation of Pax7 and MyoD expression in adult satellite cells with migration will give us more insight on how these genes can conceivably stimulate the migratory response. As for Myf5, a similar trend to MyoD was observed. However, for both MyoD and MyoG, 24 h might be too early to see any significant difference, especially for MyoG since it is a myogenic factor that is typically not upregulated until later phases of satellite cell differentiation [37].

5. CONCLUSIONS

With the overall goal of engineering a scaffold that could facilitate the migration of endogenous satellite cells into and within the scaffolds to help enhance body's regenerative response for the treatment of VML; results showed promise for the use of the 3% HA hydrogel functionalized with the laminin peptide, IKVAV. Attributions include promotion of satellite cell spreading while still enhancing cell migration, and the upregulation of transcription factors associated with the activation of satellite cells, MyoD and Pax7, for muscle repair.

While proliferation was not particularly enhanced, growth factors present at the site of injury could help mediate proliferation. Since satellite cell proliferation is highly stimulated by growth factors that are upregulated at the site of injury, including hepatocyte growth factor (HGF) and insulin-like growth factor (IGF) [52, 53]. Therefore, we expect that upon hydrogel implantation the in vivo response could stimulate proliferation to enhance the efficacy of the gels. Moreover, cell proliferation is also enhanced with the increase of cell density [11], meaning that as satellite cell number increases as a result to migration, the proliferative response would likely also increase. If the latter holds true, then differentiation and myotube formation would inherently follow.

6. APPENDIX

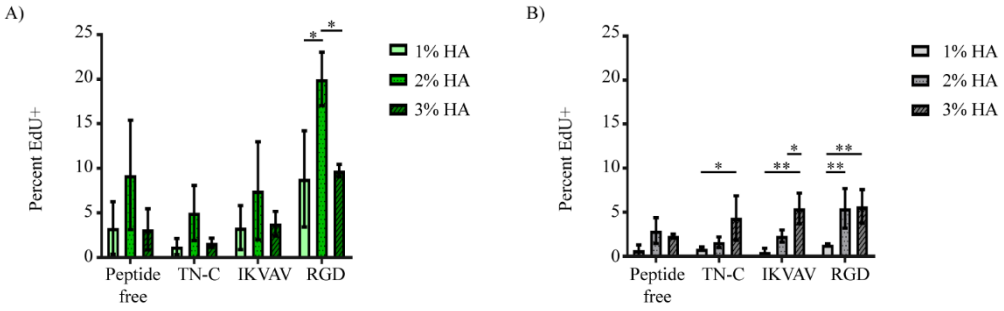

Figure 9. Comparison of total DNA synthesis between A) GFP+ and B) GFP- cells.

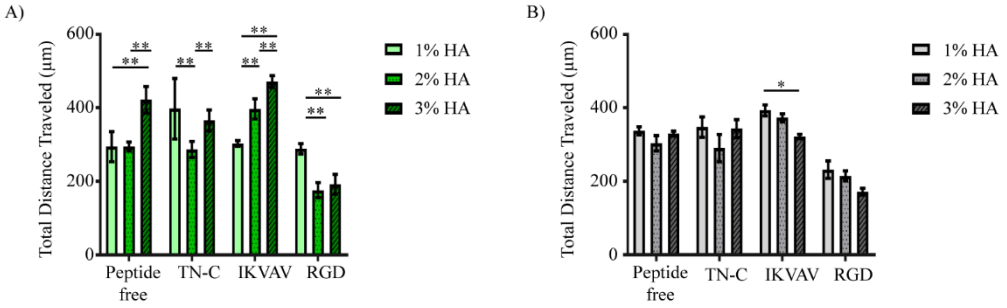

Figure 10. Total distance traveled by A) GFP+ and B) GFP-

7. REFERENCES

[1] S. Calve, S.J. Odelberg, H.-G. Simon, A transitional extracellular matrix instructs cell behavior during muscle regeneration, Developmental biology 344(1) (2010) 259-271.
[2] S. Calve, H.G. Simon, Biochemical and mechanical environment cooperatively regulate skeletal muscle regeneration, FASEB journal : official publication of the Federation of American Societies for Experimental Biology 26(6) (2012) 2538-45.
[3] K. Goetsch, K. Myburgh, C.U. Niesler, In vitro myoblast motility models: investigating migration dynamics for the study of skeletal muscle repair, J. Muscle Res. Cell Motil., 2013, pp. 333-347.
[4] S.S. Rayagiri, D. Ranaldi, A. Raven, I.F. Mohamad Azhar, O. Lefebvre, P.S. Zammit, A.G. Borycki, Basal lamina remodeling at the skeletal muscle stem cell niche mediates stem cell self-renewal, (2018).
[5] K. Boonen, M. Post, The Muscle Stem Cell Niche: Regulation of Satellite Cells During Regeneration, in: K.J.M. Boonen (Ed.) 2008, pp. 419-432.
[6] F.S. Tedesco, Repairing skeletal muscle: regenerative potential of skeletal muscle stem cells, The Journal Of Clinical Investigation 120(1) (2010) 11.
[7] A.X. Bigard, E. Fink, Skeletal Muscle Regeneration After Injury: Cellular and Molecular Events, (2008) 28-55.
[8] B. Grogan, Hsu, Jr., Volumetric Muscle Loss, J. Am. Acad. Orthop. Surg. 19 (2011) S35-S37.
[9] R. Vracko, Basal lamina scaffold-anatomy and significance for maintenance of orderly tissue structure, The American journal of pathology 77(2) (1974) 314.
[10] J.R. Sanes, The basement membrane/basal lamina of skeletal muscle, The Journal of biological chemistry 278(15) (2003) 12601.
[11] M.M. Murphy, J.A. Lawson, S.J. Mathew, D.A. Hutcheson, G. Kardon, Satellite cells, connective tissue fibroblasts and their interactions are crucial for muscle regeneration, Development 138(17) (2011) 3625.
[12] M.H. Branton, J.B. Kopp, TGF-beta and fibrosis, Microbes and infection 1(15) (1999) 1349-65.
[13] A.L. Serrano, C.J. Mann, B. Vidal, E. Ardite, E. Perdiguero, P. Muñoz-Cánoves, Cellular and Molecular Mechanisms Regulating Fibrosis in Skeletal Muscle Repair and Disease, Current Topics in Developmental Biology 96 (2011) 167-201.
[14] B.T. Corona, J.C. Rivera, J.G. Owens, J.C. Wenke, C.R. Rathbone, Volumetric muscle loss leads to permanent disability following extremity trauma, Journal of rehabilitation research and development 52(7) (2015) 785-92.
[15] K.W. VanDusen, B.C. Syverud, M.L. Williams, J.D. Lee, L.M. Larkin, Engineered skeletal muscle units for repair of volumetric muscle loss in the tibialis anterior muscle of a rat, Tissue engineering. Part A 20(21-22) (2014) 2920-30.
[16] S.I. Hodgetts, M.W. Beilharz, A.A. Scalzo, M.D. Grounds, Why do cultured transplanted myoblasts die in vivo? DNA quantification shows enhanced survival of donor male myoblasts in host mice depleted of CD4+ and CD8+ cells or Nk1.1+ cells, Cell transplantation 9(4) (2000) 489-502.

[17] C. Fuoco, L.L. Petrilli, S. Cannata, C. Gargioli, Matrix scaffolding for stem cell guidance toward skeletal muscle tissue engineering, Journal of Orthopaedic Surgery and Research 11 (2016) 86.
[18] S. Calve, J. Isaac, J.P. Gumucio, C.L. Mendias, Hyaluronic acid, HAS1, and HAS2 are significantly upregulated during muscle hypertrophy, American journal of physiology. Cell physiology 303(5) (2012) C577-88.
[19] M.N. Collins, C. Birkinshaw, Hyaluronic acid based scaffolds for tissue engineering--a review, Carbohydrate polymers 92(2) (2013) 1262-79.
[20] X.Z. Shu, Y. Liu, Y. Luo, M.C. Roberts, G.D. Prestwich, Disulfide Cross-Linked Hyaluronan Hydrogels, Biomacromolecules 3(6) (2002) 1304-1311.
[21] X. Zheng Shu, Y. Liu, F.S. Palumbo, Y. Luo, G.D. Prestwich, In situ crosslinkable hyaluronan hydrogels for tissue engineering, Biomaterials 25(7-8) (2004) 1339-48.
[22] J.W. Burns, K. Skinner, J. Colt, A. Sheidlin, R. Bronson, Y. Yaacobi, E.P. Goldberg, Prevention of Tissue Injury and Postsurgical Adhesions by Precoating Tissues with Hyaluronic Acid Solutions, Journal of Surgical Research 59(6) (1995) 644-652.
[23] X. Shu, K. Ghosh, Y. Liu, F. Palumbo, Y. Luo, R. Clark, G. Prestwich, Attachment and spreading of fibroblasts on an RGD peptide-modified injectable hyaluronan hydrogel, Journal Of Biomedical Materials Research Part A 68A(2) (2004) 365-375.
[24] U. Hersel, RGD modified polymers: biomaterials for stimulated cell adhesion and beyond, Biomaterials 24(24) (2003) 4385.
[25] W. Ning, Cellular adhesion: Instant integrin mechanosensing, Nature Materials 16(12) (2017) 1173.
[26] D. Eng, M. Caplan, M. Preul, A. Panitch, Hyaluronan scaffolds: A balance between backbone functionalization and bioactivity, Acta biomaterialia 6(7) (2010) 2407-2414.
[27] P.H.W. Butterworth, H. Baum, J.W. Porter, A modification of the Ellman procedure for the estimation of protein sulfhydryl groups, Archives of Biochemistry and Biophysics 118(3) (1967) 716-723.
[28] G.L. Ellman, A colorimetric method for determining low concentrations of mercaptans, Archives of Biochemistry and Biophysics 74(2) (1958) 443-450.
[29] U. Hersel, C. Dahmen, H. Kessler, RGD modified polymers: biomaterials for stimulated cell adhesion and beyond, Biomaterials 24(24) (2003) 4385-4415.
[30] E. Ruoslahti, RGD and other recognition sequences for integrins, Annual review of cell and developmental biology 12 (1996) 697-715.
[31] M.L. Mercado, A. Nur-e-Kamal, H.Y. Liu, S.R. Gross, R. Movahed, S. Meiners, Neurite outgrowth by the alternatively spliced region of human tenascin-C is mediated by neuronal alpha7beta1 integrin, The Journal of neuroscience : the official journal of the Society for Neuroscience 24(1) (2004) 238-47.
[32] K. Tashiro, G.C. Sephel, B. Weeks, M. Sasaki, G.R. Martin, H.K. Kleinman, Y. Yamada, A synthetic peptide containing the IKVAV sequence from the A chain of laminin mediates cell attachment, migration, and neurite outgrowth, The Journal of biological chemistry 264(27) (1989) 16174-82.
[33] K.A. Engleka, A.D. Gitler, M. Zhang, D.D. Zhou, F.A. High, J.A. Epstein, Insertion of Cre into the Pax3 locus creates a new allele of Splotch and identifies unexpected Pax3 derivatives, Developmental biology 280(2) (2005) 396-406.

[34] M. Linda, A.Z. Theresa, M.S. Susan, O. Seung Wook, A.Z. Hatim, G. Hong, L.N. Lydia, D.P. Richard, J.H. Michael, R.J. Allan, S.L. Ed, Z. Hongkui, A robust and high-throughput Cre reporting and characterization system for the whole mouse brain, Nature Neuroscience 13(1) (2009) 133.
[35] H. Mohammad, R. Syed Morteza, Z. Mehadi, D. Ehsan, Optimization of Chemically Defined Cell Culture Media for Recombinant ONTAK Immunotoxin Production, Iranian Journal of Medical Microbiology 8(3) (2014) 51-57.
[36] R.O. Hynes, Cell adhesion: old and new questions, Trends in cell biology 9(12) (1999) M33-7.
[37] J. Dhawan, T.A. Rando, Stem cells in postnatal myogenesis: molecular mechanisms of satellite cell quiescence, activation and replenishment, Trends in cell biology 15(12) (2005) 666-673.
[38] S. Oustanina, G. Hause, T. Braun, Pax7 directs postnatal renewal and propagation of myogenic satellite cells but not their specification, EMBO Journal 23(16) (2004) 3430-3439.
[39] E. Suniti, R.M. Roger, C.H. Vincent, E. Shibnath, INTERACTIONS BETWEEN HYALURONAN AND ITS RECEPTORS (CD44, RHAMM) REGULATE THE ACTIVITIES OF INFLAMMATION AND CANCER, Frontiers in Immunology 6(MAY) (2015).
[40] C.f. Bentzinger, Yu x. Wang, J. Von maltzahn, Vahab d. Soleimani, H. Yin, Michael a. Rudnicki, Fibronectin Regulates Wnt7a Signaling and Satellite Cell Expansion, Cell Stem Cell 12(1) (2013) 75-87.
[41] E. Hadjipanayi, V. Mudera, R.A. Brown, Close dependence of fibroblast proliferation on collagen scaffold matrix stiffness, Journal of Tissue Engineering and Regenerative Medicine 3(2) (2009) 77-84.
[42] K. Veit, B.-S. Beate, W. Franz, Hyaluronic acid influences the migration of myoblasts within the avian embryonic wing bud, American Journal of Anatomy 192(4) (1991) 400-406.
[43] M.D. Boppart, D.J. Burkin, S.J. Kaufman, Alpha7beta1-integrin regulates mechanotransduction and prevents skeletal muscle injury, American journal of physiology. Cell physiology 290(6) (2006) C1660.
[44] T. Boontheekul, E.E. Hill, H.J. Kong, D. Mooney, Regulating Myoblast Phenotype Through Controlled Gel Stiffness and Degradation, Tissue Engineering 13(7) (2007) 1431-1442.
[45] K. Ghosh, Z. Pan, E. Guan, S. Ge, Y. Liu, T. Nakamura, X.-D. Ren, M. Rafailovich, R.A.F. Clark, Cell adaptation to a physiologically relevant ECM mimic with different viscoelastic properties, Biomaterials 28(4) (2007) 671-679.
[46] V.P. Terranova, M. Aumailley, L.H. Sultan, G.R. Martin, H.K. Kleinman, Regulation of cell attachment and cell number by fibronectin and laminin, Journal of Cellular Physiology 127(3) (1986) 473-479.
[47] S.L. Goodman, G. Risse, K. Von Der Mark, The E8 subfragment of laminin promotes locomotion of myoblasts over extracellular matrix, The Journal of Cell Biology 109(2) (1989) 799-809.
[48] J. Huijbregts, J.D. White, M.D. Grounds, The absence of MyoD in regenerating skeletal muscle affects the expression pattern of basement membrane, interstitial matrix and integrin molecules that is consistent with delayed myotube formation, Acta Histochemica 103(4) (2001) 379-396.
[49] E. Brzóska, V. Bello, T. Darribère, J. Moraczewski, Integrin α3 subunit participates in myoblast adhesion and fusion in vitro, Differentiation 74(2-3) (2006) 105-118.

[50] O. Sacco, M. Silvestri, F. Sabatini, R. Sale, A.-C. Defilippi, G.A. Rossi, Epithelial cells and fibroblasts: structural repair and remodelling in the airways, Paediatric respiratory reviews 5 Suppl A (2004) S35.
[51] F. Relaix, D. Rocancourt, A. Mansouri, M. Buckingham, Divergent functions of murine Pax3 and Pax7 in limb muscle development, Genes & Development 18(9) (2004) 1088-1105.
[52] S.S. M., T. Ryuichi, T.-G.C. J., A.R. E., HGF is an autocrine growth factor for skeletal muscle satellite cells in vitro, Muscle & Nerve 23(2) (2000) 239-245.
[53] S. Machida, Insulin-like growth factor 1 and muscle growth: implication for satellite cell proliferation, The Proceedings Of The Nutrition Society 63(2) (2004) 337.